Supplemental material

Loyher et al., https://doi.org/10.1084/jem.20180534

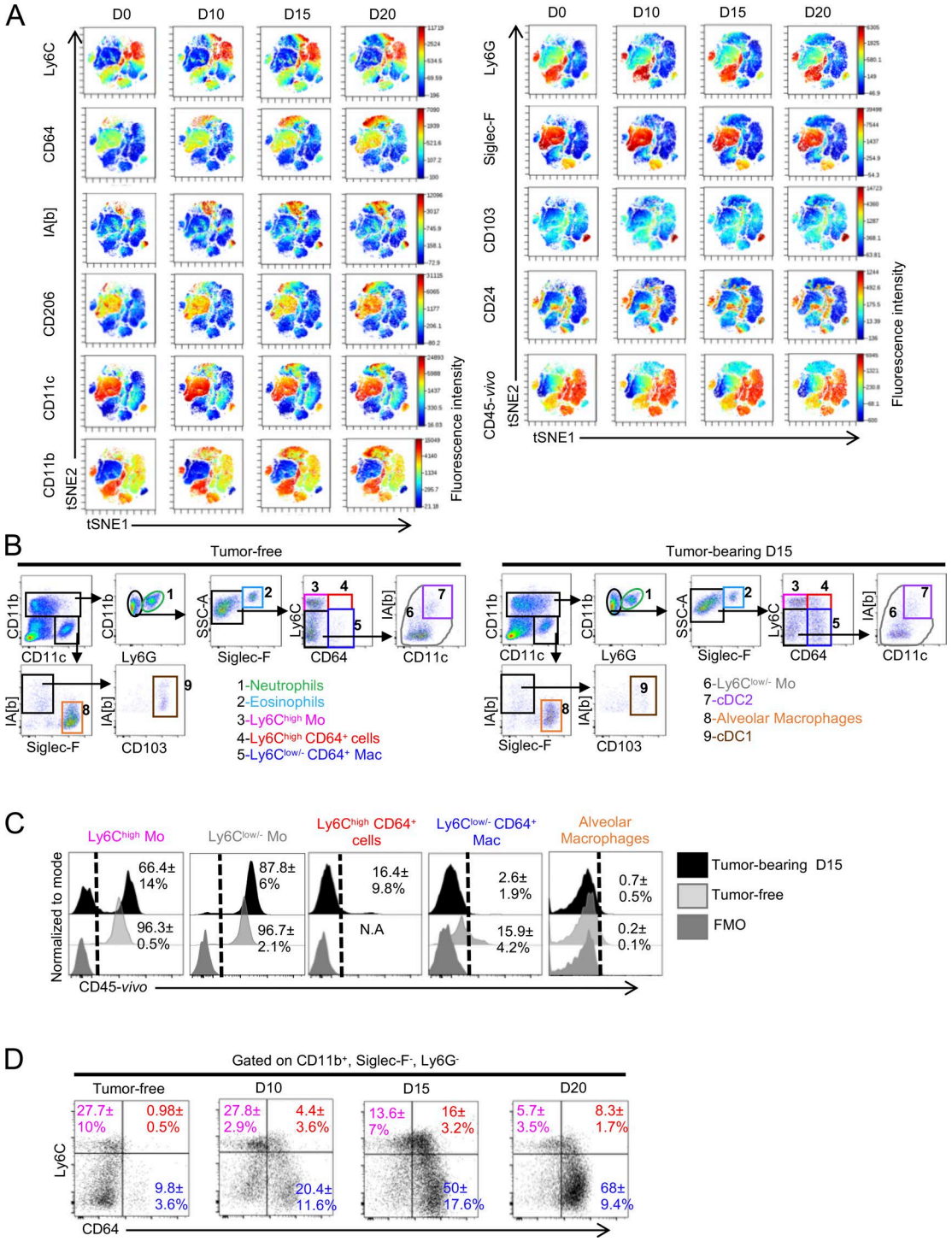

Figure S1. **Lung macrophage subsets differentially accumulate during tumor development (related to Fig. 1). (A)** tSNE dimension 1 and 2 plots of the lung myeloid compartment show relative expression intensity of each indicated phenotypic marker at different time point after TC-1 cell intravenous inoculation. **(B)** Flow cytometry dot plots of CD45+ cells show the gating strategy to discriminate lung myeloid cells in tumor-free and tumor-bearing animals. **(C)** Representative histogram plots show in vivo CD45 labeling by blood/tissue partitioning of each indicated subsets in tumor-free and tumor-bearing mice. (Mean percentage ± SD of in vivo CD45+ cells are indicated). **(D)** Dot plots show Ly6C and CD64 expressions by CD11b+Siglec-F-Ly6G- lung cells over time after tumor inoculation. Mean percentage ± SD of cells in each gate are indicated; *n* = 6–8 mice per time point out three independent experiments.

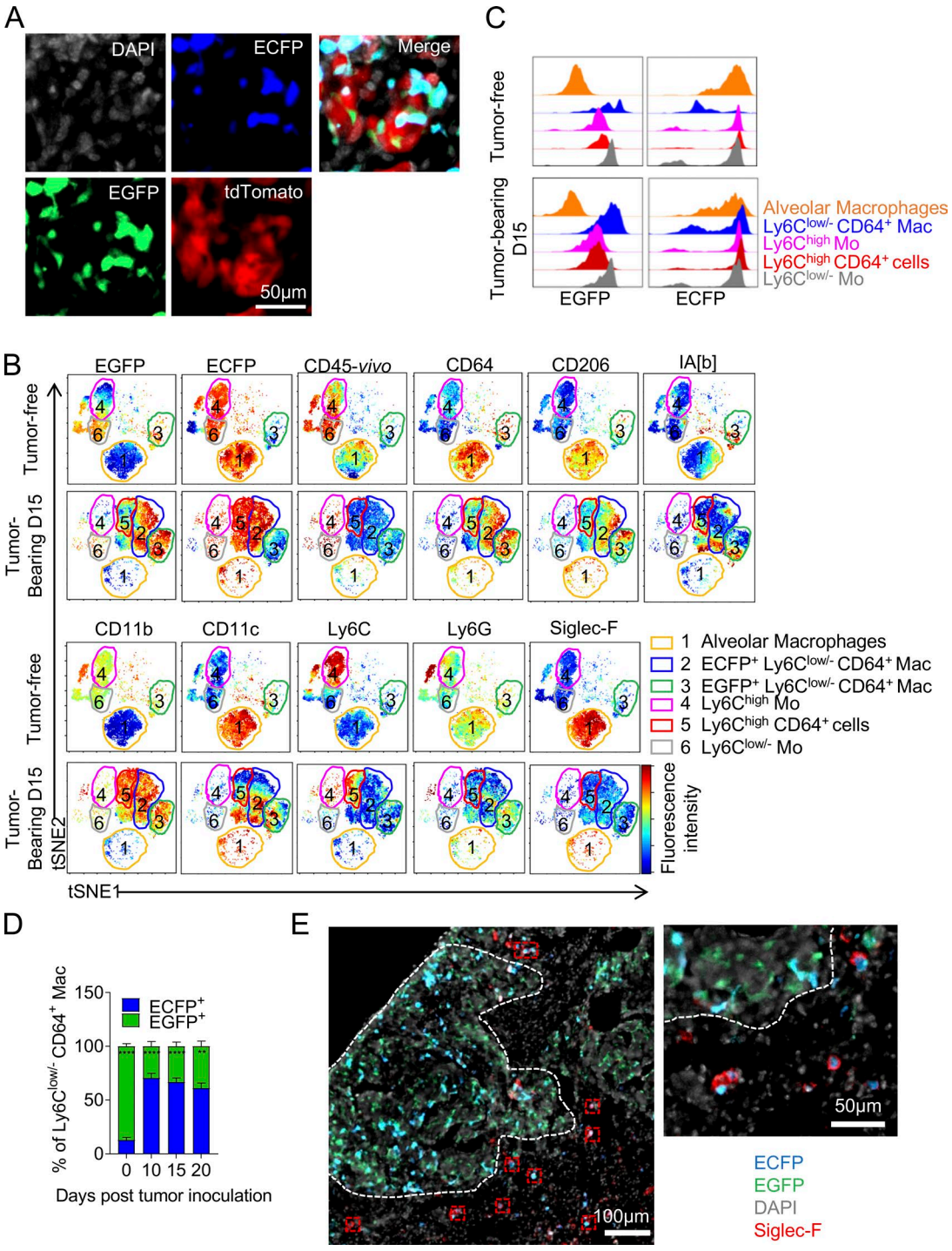

Figure S2. **Macrophages have distinct origins within lung tumors (related to Fig. 2). (A)** Lung cryo-sections from TC-1 tumor-bearing MacBlue × *Cx3cr1*$^{EGFP/+}$ show typical single channel images. **(B)** Unsupervised tSNE dimension 1 and 2 analyses indicate the myeloid cell subset clustering according to the relative expression intensity of each indicated phenotypic markers in tumor-free and TC-1 tumor-bearing MacBlue × *Cx3cr1*$^{EGFP/+}$ mice at day 15. **(C)** Histogram plots of EGFP and ECFP expression in indicated myeloid subsets in tumor-free and TC-1 tumor-bearing MacBlue × *Cx3cr1*$^{EGFP/+}$ mice at day 15. **(D)** Graph shows the relative proportion of EGFP$^+$ and ECFP$^+$ Ly6C$^{low/-}$CD64$^+$ Mac (bars represent mean ± SEM from 6–10 mice out of three independent experiments). **(E)** Lung cryo-sections from TC-1 tumor-bearing MacBlue × *Cx3cr1*$^{EGFP/+}$ were stained with anti–Siglec-F and show ECFP$^+$ Siglec-F$^+$ AM exclusion from tumor nodules. For all panels: **, P < 0.01; ****, P < 0.0001.

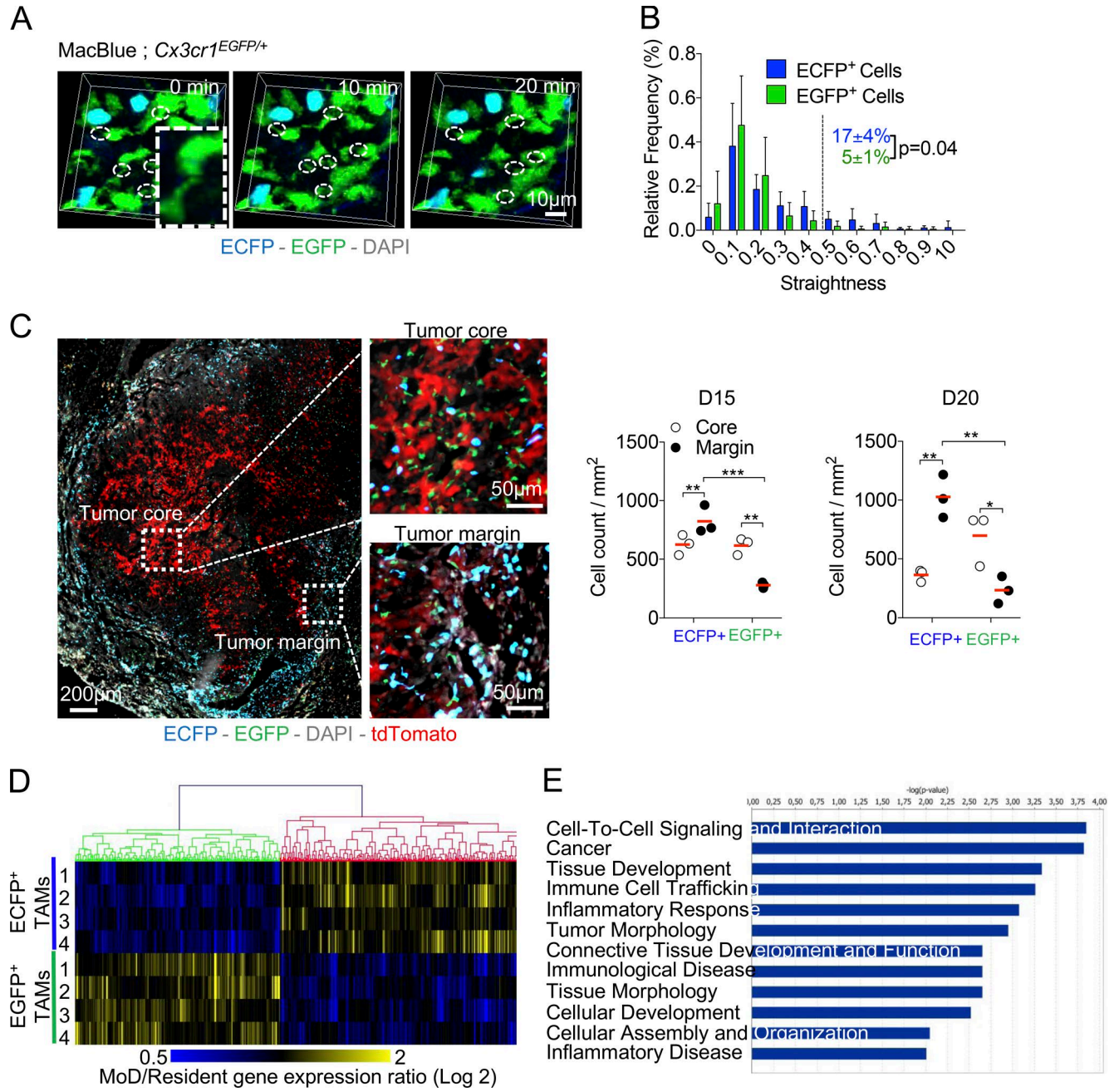

Figure S3. **Resident and MoD-TAMs harbor distinct phenotypes and anatomical distribution (related to Fig. 4). (A)** Time-lapse TPLSM image sequence showing the dynamic of resident EGFP⁺-TAM interactions (dashed circles). Dashed box is a 2.5× zoom-in of the picture showing cell interaction **(B)** Graph represents the relative distribution of track straightness of ECFP⁺ and EGFP⁺ cells in lung tumors at day 15, and the proportion of cells above the threshold are indicated (dashed line). Bars represent mean ± SEM from four mice out of two independent experiments; Mann-Whitney tests were performed. See also Videos 1 and 2. **(C)** Lung cryo-sections from TC-1^{tdTomato} tumor-bearing MacBlue × *Cx3cr1*$^{EGFP/+}$ show ECFP⁺ and EGFP⁺ cell distribution at the progressing front of lung nodules at day 20. Graphs show quantifications of ECFP⁺ and EGFP⁺ cells in the tumor core or at the tumor margin. Mice are pooled from two independent experiments; red bars indicate means. **(D)** Hierarchical clustering of differentially regulated transcripts distinguishes MoD-TAMs and Res-TAMs sorted from lung tumors 20 d after TC-1 inoculation (n = 4 independent cell preparation in each group, each sorting was performed from a pool of two to three mice). **(E)** Enriched function groups that distinguished MoD-TAMs and Res-TAMs based on Ingenuity Pathways Analysis with a P value cut-off <0.01. For all panels: *, P < 0.05; **, P < 0.01; ***, P < 0.001.

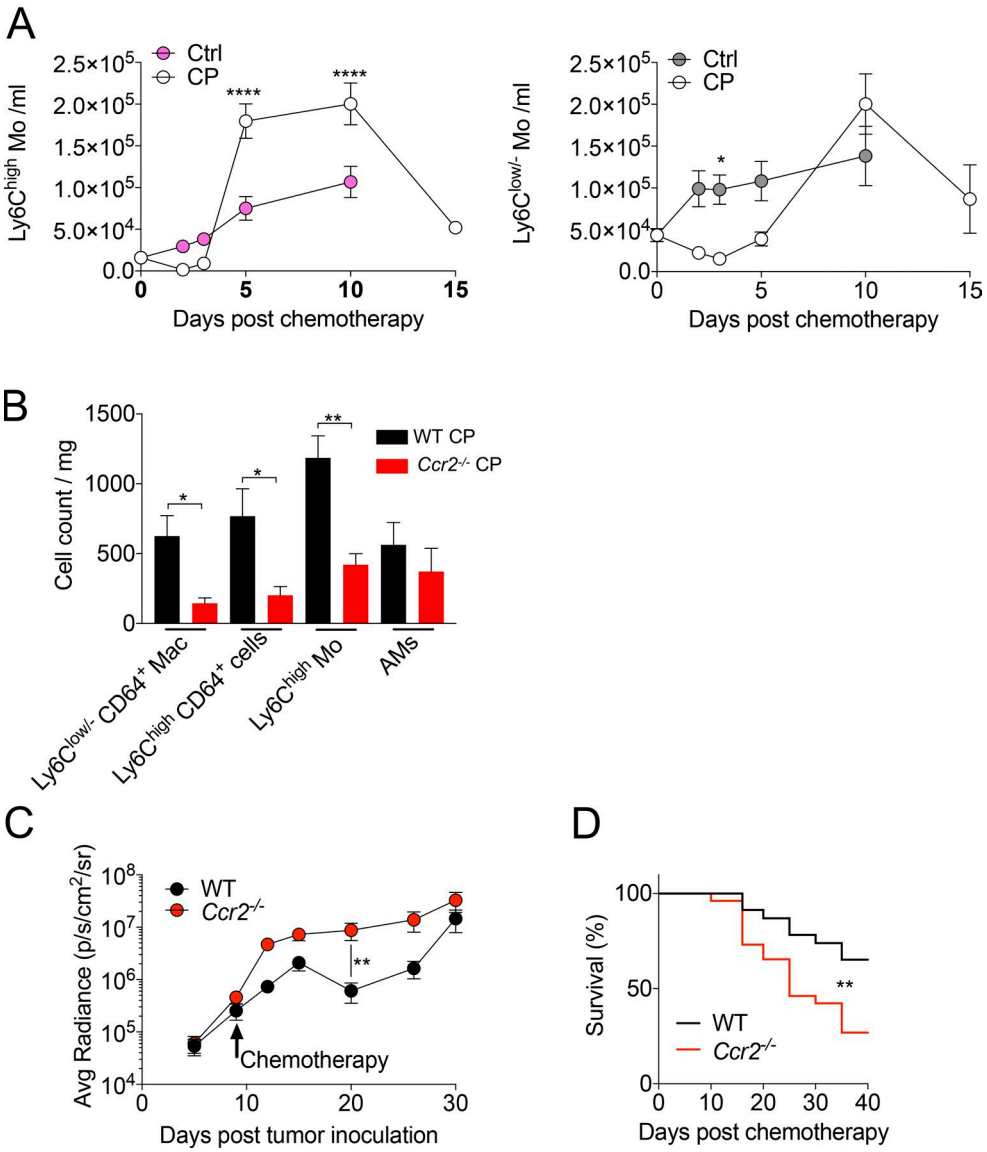

Figure S4. **Distinct sensitivity and recovery of Res-TAMs and MoD-TAMs after chemotherapy (related to Fig. 6). (A)** Graphs represent the kinetic of Ly6C^{high}-Mo and Ly6C$^{low/-}$-Mo recovery in the blood, after CP treatment (mean absolute number/milliliter of blood ± SEM are represented; *n* = 6–10 mice out of two to four independent experiments; two-way ANOVA with Bonferroni multiple comparisons test was performed; only statistical differences compared with day 0 after chemotherapy are indicated for each compartment). **(B)** Graph shows the absolute number per milligram of tissue of indicated population 15 d after tumor inoculation in WT and *Ccr2*$^{-/-}$ mice treated with CP (bars represent mean ± SEM from 10 mice out of three independent experiments; two-way ANOVA with Bonferroni multiple comparisons test was performed). **(C)** Graph represents the monitoring of tumor growth by bioluminescence imaging after treatment in TC-1-Luc tumor-bearing WT and *Ccr2*$^{-/-}$ mice (*n* = 10 mice per group pooled from two independent experiments). **(D)** Survival curve of WT mice and *Ccr2*$^{-/-}$ mice after TC-1 inoculation and CP treatment (*n* = 23–26 mice per group, pooled from four experiments; log-rank [Mantel-Cox] test was performed). For all panels: *, P < 0.05; **, P < 0.01; ****, P < 0.0001.

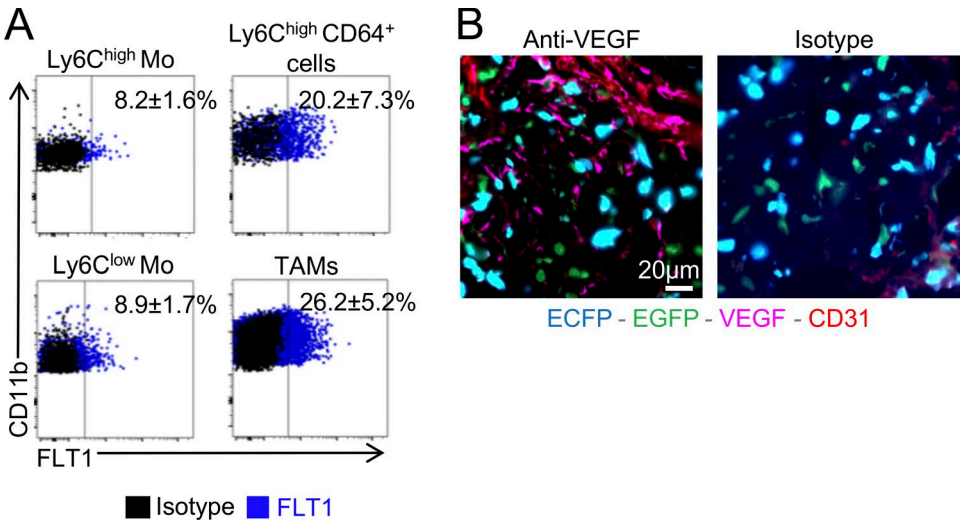

Figure S5. **Anti-VEGF targets Res-TAM and MoD-TAM accumulation (related to Fig. 8). (A)** Dot plots show the expression of FLT1 (VEGF receptor 1) on the indicated subsets. Isotype control staining is overlaid in black. Percentage ± SD is indicated; *n* = 8 mice. **(B)** Lung cryo-sections from tumor-bearing MacBlue × *Cx3cr1*$^{EGFP/+}$ mouse show TAM distribution regarding the expression of VEGF in tumor nodules. Anti-VEGF isotype staining is represented (right image). Data are representative of two independent experiments.

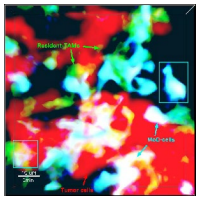

Video 1. **Live imaging of TAM subsets in lung tumors (related to Fig. 4).** 3D live imaging video shows the behaviors of EGFP$^+$ (green) and ECFP$^+$ (cyan) in explanted lung of MacBlue × *Cx3cr1*$^{EGFP/+}$ mouse 15 d after TC-1^{tdtomato} cell inoculation (red). Notice the dynamics of ECFP$^+$ cells (cyan squares) and the interactions between EGFP$^+$ macrophages (white circles).

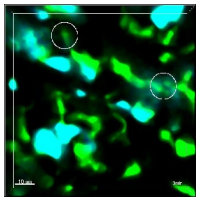

Video 2. **Live imaging of EGFP$^+$-TAM interactions in lung tumors (related to Fig. 4).** 3D live imaging video shows the dynamic protrusions (white circles) of EGFP$^+$ cells (green) in explanted lung of MacBlue × *Cx3cr1*$^{EGFP/+}$ mouse 15 d after TC-1 cell inoculation.